Journal of Analytical Toxicology, 2020;44:226–236

Article

In Vitro Metabolic Profile Elucidation of Synthetic Cannabinoid APP-CHMINACA (PX-3)

Brandon C. Presley[1,*], Barry K. Logan[2] and Susan A. Jansen-Varnum[1]

[1]Department of Chemistry, Temple University, 1901 N. 13th St., Philadelphia, PA 19122, USA and [2]The Center for Forensic Science Research and Education, Fredric Rieders Family Foundation, 2300 Stratford Ave., Willow Grove, PA 19090, USA

*Author to whom correspondence should be addressed. Email: brandon.presley@temple.edu

Abstract

Indazole carboxamide synthetic cannabinoids remain the most prevalent subclass of new psychoactive substances (NPS) reported internationally. However, the metabolic and pharmacological properties of many of these compounds remain unknown. Elucidating these characteristics allows members of the clinical and forensic communities to identify causative agents in patient samples, as well as render conclusions regarding their toxic effects. This work presents a detailed report on the *in vitro* phase I metabolism of indazole carboxamide synthetic cannabinoid APP-CHMINACA (PX-3). Incubation of APP-CHMINACA with human liver microsomes, followed by analysis of extracts via high-resolution mass spectrometry, yielded 12 metabolites, encompassing 7 different metabolite classes. Characterization of the metabolites was achieved by evaluating the product ion spectra, accurate mass and chemical formula generated for each metabolite. The predominant biotransformations observed were hydrolysis of the distal amide group and hydroxylation of the cyclohexylmethyl (CHM) substituent. Nine metabolites were amide hydrolysis products, of which five were monohydroxylated, one dihydroxylated and two were ketone products. The metabolites in greatest abundance in the study were products of amide hydrolysis with no further biotransformation (M1), followed by amide hydrolysis with monohydroxylation (M2.1). Three APP-CHMINACA-specific metabolites were generated, all of which were hydroxylated on the CHM group; one mono-, di- and tri-hydroxylated metabolite each was produced, with dihydroxylation (M6) present in the greatest abundance. The authors propose that metabolites M1, M2.1 and M6 are the most appropriate markers to determine consumption of APP-CHMINACA. The methods used in the current study have broad applicability and have been used to determine the *in vitro* metabolic profiles of multiple synthetic cannabinoids and other classes of NPS. This research can be used to guide analytical scientists in method development, synthesis of reference material, pharmacological testing of proposed metabolites and prediction of metabolic processes of compounds yet to be studied.

Introduction

New psychoactive substances (NPSs) are compounds that were originally purposed for medicinal chemistry research but have appeared in seized drug materials and biological specimens submitted to forensic laboratories over the past decade (1–5). In many instances, the compounds were previously reported in pharmaceutical patents and academic literature; however, they are presently sold online and covertly in smoke shops around the world (6, 7). Chemical classes of NPS include but are not limited to synthetic cannabinoids, phenethylamine derivatives, synthetic opioids, designer benzodiazepines and synthetic cathinones (2, 8, 9). According to the United Nations Office on Drugs and Crime (UNODC), between 2008 and March 2019, 119 countries and territories submitted a cumulative total of 899

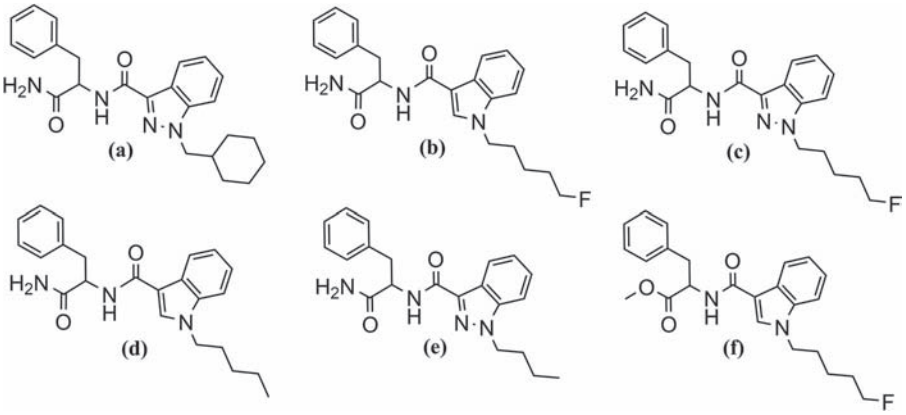

Figure 1. Chemical structures of synthetic cannabinoids: APP-CHMINACA (PX-3) (a), 5-fluoro APP-PICA (PX-1) (b), 5-fluoro APP-PINACA (PX-2) (c), APP-PICA (d), APP-BINACA (e) and 5-fluoro MPP-PICA (f).

individual NPS identifications, of which synthetic cannabinoids were the most reported substance class (10). Indazole carboxamide-type synthetic cannabinoids remain the most abundant subclass reported internationally, based on the number of compounds identified in forensic and clinical casework (2, 5, 8, 11–13). Synthetic cannabinoids have the potential to bind to and activate cannabinoid receptor type-1 (CB_1) and type-2 (CB_2), producing effects that mimic those of Δ^9-tetrahydrocannabinol (THC), the primary psychoactive component present in cannabis. Many indazole carboxamides are potent receptor agonists, however, and induce severe physiological effects, more harmful than those exhibited when THC is consumed (14–18).

APP-CHMINACA (Figure 1a), *N*-(1-amino-1-oxo-3-phenylpropan-2-yl [APP])-1-(cyclohexylmethyl [CHM])-1*H*-indazole-3-carboxamide [INACA] (common name: PX-3), is a synthetic cannabinoid of the indazole carboxamide class (2). Indazole carboxamide synthetic cannabinoids are classified based on their indazole core ring structure and carboxamide linking group. The carboxamide group in APP-CHMINACA links the indazole ring system to an APP moiety. The indazole group is substituted at the 1-position with a CHM ring, a common substituent of highly potent synthetic cannabinoids (19, 20).

APP-CHMINACA was originally reported by Pfizer in a 2009 patent as a cannabinoid receptor ligand being studied for potential therapeutic benefits; it is referred to as "Example 14" in the patent (21). The CB_1 and CB_2 binding affinity (K_i) and receptor activation ability of APP-CHMINACA relative to [^{3}H] CP 55,940 (a full agonist at both receptors), and THC was evaluated by Schoeder *et al.* (20). Receptor binding studies were performed via a radioligand binding assay, while activation was assessed through a cyclic adenosine monophosphate (cAMP) accumulation assay. K_i values of 9.81 nM at CB_1, and 4.39 nM at CB_2 were determined for APP-CHMINACA; for [^{3}H] CP 55,940: 1.28 nM (CB_1), 1.42 nM (CB_2) and THC: 3.87 nM (CB_1), 71.6 nM (CB_2). In the cAMP study, APP-CHMINACA activated both receptors at a concentration of 1 μM. Activation at CB_1 and CB_2 was approximately 75% and 90% (respectively) of the values obtained by [^{3}H] CP 55,940, demonstrating its agonistic properties. Both receptors were activated by APP-CHMINACA to a greater degree than THC (20).

Doi *et al.* conducted pharmacological evaluations of the (*R*)- and (*S*)-enantiomers of APP-CHMINACA to assess the degree to which each molecule activated the CB receptors; activation was determined via a [^{35}S] guanosine 5′-O-[gamma-thio] triphosphate (GTPγS) binding assay (22). The concentrations of the APP-CHMINACA enantiomers at which the activation response was 50% of the response of the normalization compound (EC_{50}) and was determined through this assay; the normalization compound utilized was [^{3}H] CP 55,940. The study revealed that (*S*)-APP-CHMINACA functions as an agonist at CB_1 (EC_{50}, 0.251 μM), while (*R*)-APP-CHMINACA (EC_{50}, 33.7 μM) did not sufficiently activate the CB_1 receptor; the (*S*)-enantiomer was 134 times more potent than the (*R*)-enantiomer at CB_1. At CB_2, (*S*)-APP-CHMINACA (EC_{50}, 8.09 nM) demonstrated agonistic properties and was approximately 61 times more potent than the (*R*)-enantiomer (EC_{50}, 0.490 μM). The results showed that the (*S*)-enantiomer of APP-CHMINACA has a greater ability to activate cannabinoid receptors than its (*R*)-isomer and preferentially activates CB_2 over CB_1. While (*S*)-APP-CHMINACA did activate the receptors, it did so to a lesser degree than the normalization compound ([^{3}H] CP 55,940). In the study, [^{3}H] CP 55,940, produced the following results: EC_{50} value of 1.28 nM at CB_1; EC_{50} of 0.154 nM at CB_2, with potencies approximately 196 and 53 times greater than (*S*)-APP-CHMINACA, at CB_1 and CB_2, respectively (22). Antonides *et al.* also performed pharmacological evaluations of (*R*)- and (*S*)-isomers of indazole carboxamide synthetic cannabinoids to assess their relative potencies at CB_1 and CB_2 (11). The authors tested AMB-FUBINACA (FUB-AMB), 5-fluoro ADB, AB-FUBINACA and AB-CHMINACA and found that the (*S*)-isomers were more potent than the (*R*)-isomers at both receptors and preferentially activated CB_2 over CB_1.

APP-CHMINACA (PX-3) is a member of the "PX-series" of synthetic cannabinoids, which includes 5-fluoro APP-PICA (PX-1) and 5-fluoro APP-PINACA (PX-2) (Figure 1b and c); APP-PICA (Figure 1d), the non-fluorinated version of PX-1, is also similar in structure to these compounds. The main structural difference between APP-CHMINACA, PX-1 and PX-2 is the presence of the CHM ring versus a fluoropentyl side chain; additionally, PX-1 and APP-PICA possess an indole core, while PX-2 bears an indazole. APP-CHMINACA is the most potent of the PX-series compounds, according to the study conducted by Schoeder *et al.* (20).

APP-CHMINACA in powdered form was identified in a package labeled "white pigments" seized by Belgian customs authorities that originated from China. The material was analyzed via gas chromatography–mass spectrometry, high-resolution mass spectrometry (HRMS), nuclear magnetic resonance (NMR) and Raman and Fourier transform-infrared (FT-IR) spectroscopies. Another indazole

Table I. Table of metabolites identified and associated biotransformations, average retention time (min), elemental composition, measured accurate mass (m/z), mass error (ppm), diagnostic product ions, and rank (based on relative peak area percent)

Metabolite ID	Biotransformation	Retention time (min)	Elemental composition	Measured accurate mass (m/z)	Mass error (ppm)	Diagnostic product ions	Rank
Parent	N/A	9.53	$C_{24}H_{28}N_4O_2$	405.2286	0.3	145, 241, 360	N/A
M1	Distal amide hydrolysis	9.81	$C_{24}H_{27}N_3O_3$	406.2130	1.3	145, 241, 360	1
M2.1	Distal amide hydrolysis and monohydroxylation (CHM)	7.83	$C_{24}H_{27}N_3O_4$	422.2074	0.0	145, 257, 376	2
M2.2	Distal amide hydrolysis and monohydroxylation (CHM)	8.00	$C_{24}H_{27}N_3O_4$	422.2074	−0.1	145, 239, 404	4
M2.3	Distal amide hydrolysis and monohydroxylation (CHM)	8.19	$C_{24}H_{27}N_3O_4$	422.2073	−0.3	145, 257, 376	5
M2.4	Distal amide hydrolysis and monohydroxylation (CHM)	8.44	$C_{24}H_{27}N_3O_4$	422.2069	−1.4	145, 257, 376	7
M2.5	Distal amide hydrolysis and monohydroxylation (CHM)	8.54	$C_{24}H_{27}N_3O_4$	422.2074	−0.1	145, 239, 404	3
M3.1	Distal amide hydrolysis and ketone (CHM) formation	7.96	$C_{24}H_{25}N_3O_4$	420.1915	−0.7	145, 255, 374	9
M3.2	Distal amide hydrolysis and ketone (CHM) formation	8.04	$C_{24}H_{25}N_3O_4$	420.1921	0.7	145, 255, 374	6
M4	Distal amide hydrolysis and dihydroxylation (CHM)	7.36	$C_{24}H_{27}N_3O_5$	438.2024	0.1	145, 273, 420	8
M5	Monohydroxylation (CHM)	7.43	$C_{24}H_{28}N_4O_3$	421.2234	0.0	145, 257, 376	12
M6	Dihydroxylation (CHM)	6.62	$C_{24}H_{28}N_4O_4$	437.2183	−0.1	145, 273, 392	10
M7	Trihydroxylation (CHM)	6.47	$C_{24}H_{28}N_4O_5$	453.2133	0.1	145, 289, 408	11

carboxamide synthetic cannabinoid, 5F-AMB, was also identified in material contained in this package (23). The National Forensic Laboratory of Slovenia performed analyses of APP-CHMINACA on material submitted in September 2015 and compiled a monograph of the data for use by forensic scientists; in addition to technologies previously mentioned, this report also included analysis via ion chromatography, GC-IR and attenuated total reflectance FT-IR spectroscopy (24). APP-CHMINACA was identified in drug and paraphernalia samples collected from patients involved in an outbreak of synthetic cannabinoid-facilitated adverse events in Anchorage, Alaska (USA) between July 2015 and May 2016; the occurrence, lasting 245 days, involved a total of 1,351 emergency department visits (25). Evaluations of the stability, recovery and detection of APP-CHMINACA in biological matrices, including serum/plasma for method development have also been performed (26, 27).

All three PX-series compounds were identified in seized drug casework in 2015, as reported by the United States Drug Enforcement Administration (DEA), totaling 65 identifications (28). PX-1 was identified in a laboratory in Sweden and reported to the European Monitoring Center for Drugs and Drug Addiction in 2014 (29); it was also reported by the DEA in its 2017 annual report on findings submitted by forensic chemistry testing laboratories in the USA (30). PX-1 was identified in biological specimens collected from intoxicated individuals who presented to an emergency department in Turkey between 2017 and 2018 (31). PX-2 (also termed PPA(N)-2201) was extracted from seized material and characterized by Qian *et al.* (32). Recent reports (2018–2019) on the identifications of PX-series synthetic cannabinoids have been compiled by the UNODC Early Warning Advisory on NPS (33).

Historically, PX-series synthetic cannabinoids were not as prevalent in forensic casework as other drug classes. However, structurally related compounds are emerging and have been identified in drug seizures and biological specimens; these compounds include the indazole carboxamide APP-BINACA (also termed APP-BUTINACA) and the indole carboxamide 5-fluoro MPP-PICA (5F-MPP-PICA) (Figure 1e and f). APP-BINACA has a butyl side chain and shares the APP group with APP-CHMINACA, while 5F-MPP-PICA possesses a terminal methyl ester and a fluoropentyl side chain. APP-BINACA was detected in postmortem blood samples in the state of Indiana (USA), and 5F-MPP-PICA was identified in a drug sample submitted by the United States Department of Homeland Security; both compounds were reported in early 2019 by The Center for Forensic Science Research and Education via their NPS Discovery platform (34, 35). Of the PX-series and structurally related compounds described here, the metabolic profile of several has not yet been determined; however, the authors of the current study recently studied the metabolism of PX-1 and have proposed the main metabolic products of APP-BINACA and 5F-MPP-PICA.

In this study, the *in vitro* metabolism of APP-CHMINACA (PX-3) was elucidated. This was accomplished by incubation of the parent molecule with human liver microsomes (HLM) and analyzing resulting incubate extracts via ultra-high performance liquid chromatography–quadrupole time of flight mass spectrometry (UHPLC-QTOF-MS). The metabolites were characterized by examining the product ion spectra and accurate masses generated by QTOF-MS and evaluation of the chemical formula produced. This manuscript provides a detailed description of the metabolic profile and proposed markers of human consumption of APP-CHMINACA.

Experimental

The materials and methods used to conduct this study are similar to those used by the authors in previous investigations; these were reported in manuscripts describing the metabolic profile

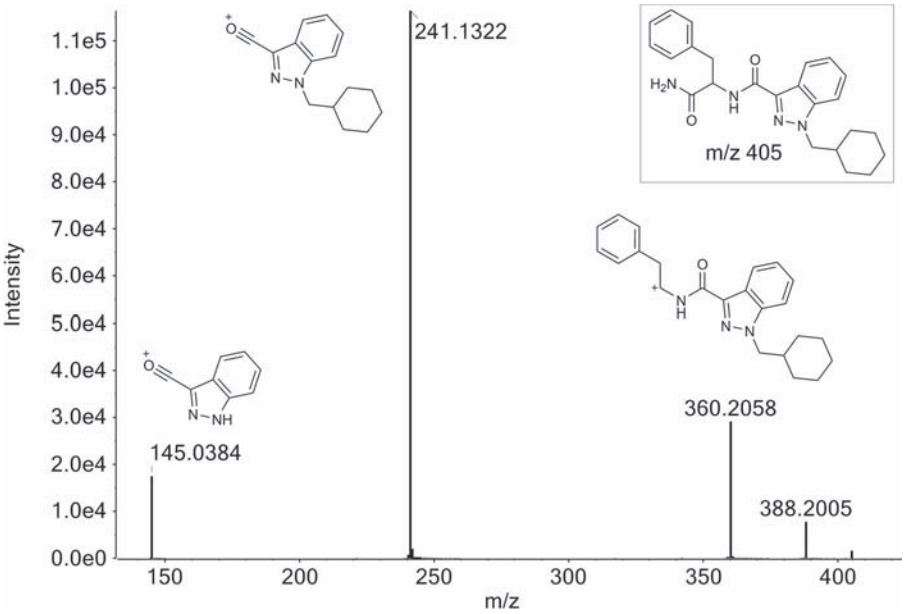

Figure 2. Product ion spectrum and chemical structures of APP-CHMINACA (top right) and fragment ions.

determination of synthetic cannabinoids PX-1 and MDMB-CHMINACA (36, 37).

Reference material, chemicals and reagents

APP-CHMINACA reference material (neat solid; ≥98% purity) and nicotinamide adenine dinucleotide phosphate (NADPH) sodium salt were obtained from Cayman Chemical (Ann Arbor, MI, USA). Diazepam standard solution (1 mg/mL; 99.9% purity) was purchased from Cerilliant® Corporation (Round Rock, TX, USA). Pooled HLM (Gibco®, 50-donors, 20 mg/mL protein concentration) and liquid chromatography–mass spectrometry (LC–MS) grade formic acid (Pierce™, >99% purity) were sourced from Thermo Fisher Scientific (Waltham, MA, USA). Sodium phosphate monobasic (monohydrate), sodium phosphate dibasic (anhydrous) and magnesium chloride (hexahydrate) (ACROS Organics) were purchased from Fisher Scientific (Waltham, MA, USA). LC–MS grade water and acetonitrile were acquired from Honeywell (Morris Plains, NJ, USA). Ammonium formate (Alfa Aesar), aqueous sodium hydroxide (BDH®, 10 *N*) and Costar® Spin-X® centrifuge tube filters (Corning®, 0.45 µm pore size) were obtained from VWR™ International (Radnor, PA).

HLM incubation procedure

A 1 mg/mL stock standard of APP-CHMINACA was prepared along with additional reagents, including 100 mM phosphate buffer (pH 7.4) with 10 mM $MgCl_2$ and 10 mM NADPH solution in LC-MS grade water. HLMs were kept frozen at −80°C prior to thawing for immediate use in experiments. APP-CHMINACA and diazepam standards were dried down under nitrogen using a Turbovap® and reconstituted in a 1:1 (v/v) mixture of phosphate buffer:acetonitrile.

Drug reaction mixtures contained APP-CHMINACA standard (5 µL) (final substrate concentration of 21 µM), phosphate buffer (520 µL), microsomes (25 µL) and NADPH solution (50 µL); the final volume of each incubate was 600 µL. Two control samples were analyzed with each drug incubation set. The first was a mixture of APP-CHMINACA standard (5 µL) and phosphate buffer (595 µL), with no addition of NADPH solution or microsomes; the purpose of this control sample was to rule out the possibility of non-enzymatic hydrolysis facilitated by the buffer solution. The second was comprised of APP-CHMINACA standard (5 µL), phosphate buffer (570 µL) and microsomes (25 µL) but no NADPH solution; this sample was implemented to examine the production of any metabolites in the presence of microsomal enzymes but absence of NADPH. All samples were prepared in glass test tubes. Prepared samples were thoroughly vortex mixed and placed into a shaking water bath set to 37°C for 2 hours. A diazepam control incubation set (prepared identically to APP-CHMINACA samples) was run in parallel to verify the enzymatic activity of the microsomes and functionality of the method. Nordiazepam, oxazepam and temazepam (representative diazepam metabolites) were screened to confirm that metabolism occurred during the incubation process. All analyses in the study were performed in duplicate.

Incubations were quenched by adding 500 µL of LC–MS grade acetonitrile, followed by vortex mixing. Samples were subsequently transferred to microcentrifuge tubes and centrifuged at 10,000 × *g* for 5 minutes. The supernatants were transferred to test tubes and dried down to ~50% of the original volume under nitrogen in a Turbovap®. The samples were then transferred to Costar® Spin-X® tubes containing filters and centrifuged at 10,000 × *g* for 5 minutes. As a final step, samples were transferred to autosampler vials for instrumental analysis.

Analysis of extracts via UHPLC-QTOF-MS: parameters and data processing criteria

HLM incubation extracts were analyzed on a Shimadzu (Kyoto, Japan) Nexera XR UHPLC system, interfaced with a Sciex (Framingham, MA, USA) TripleTOF® 5600+ QTOF mass spectrometer. Metabolites were separated chromatographically using a Kinetex C18 column, 50 × 3.0 mm, 2.6 µm (Phenomenex®, Torrance, CA,

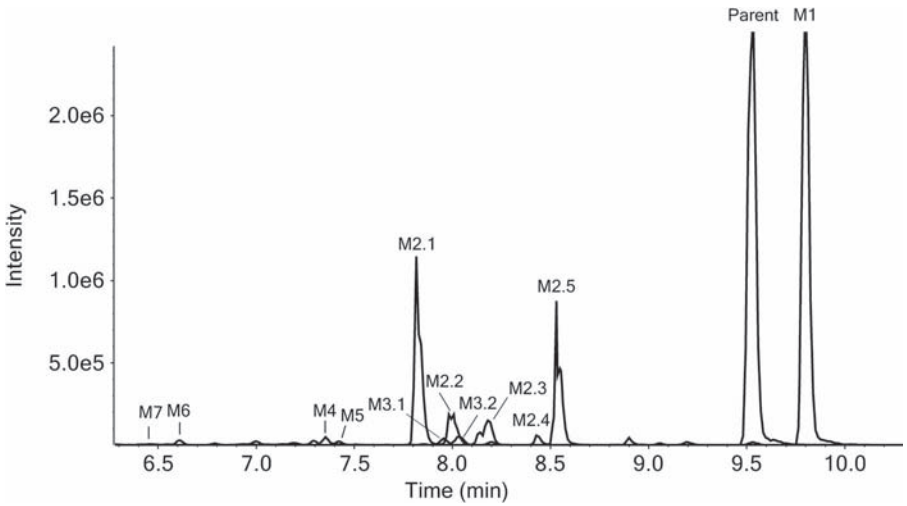

Figure 3. Extracted ion chromatogram of metabolites identified.

USA) with a column temperature set to 30°C. Mobile phase A (MPA) consisted of 10 mM ammonium formate (pH 3) in LC–MS grade water; mobile phase B (MPB) was composed of 0.1% formic acid in 50:50 methanol:acetonitrile. A linear gradient of 95:5 MPA:MPB to 5:95 (after 13 minutes) and back to 95:5 was applied. A flow rate of 0.4 mL/min was used, with a sample injection volume of 10 µL. The total run time was 15.5 minutes.

The QTOF was operated in positive electrospray ionization mode (+ESI). The source parameters were the following: source temperature, 600°C; ion spray voltage, 2500 V; declustering potential, 80 V; curtain gas, 30 psi; gas 1, 50 psi; gas 2, 50 psi. Precursor ion accurate masses were measured using a TOF-MS scan (m/z 100–1000); they were then fragmented using a 35 ± 15 eV collision energy spread to generate product ions (scan range of m/z 40–1000). Mass spectral data were acquired in information-dependent acquisition mode using Analyst® TF software (Sciex, Version 1.7); the 16 most abundant ions were isolated during each cycle with a minimum of 100 counts per second (cps) and subsequently underwent dependent MS-MS scan. A calibration solution was injected throughout the run (every five injections) to maintain mass axis calibration.

MetabolitePilot™ (Sciex, Version 1.5) and PeakView® (Sciex, Version 2.2) software were used to characterize and verify metabolites, respectively. MetabolitePilot™ data were generated based on pre-selected parameters, common for elucidation of metabolites including mass defect filtering (50 mDa), isotope pattern (intensity tolerance of 20%; MS m/z tolerance of 3 mDa), characteristic product ions and neutral losses (minimum of 1 each), common biotransformations (e.g., mono/di/trihydroxylation, hydrolysis etc.; total of 60 selected), number of allowed bond breakages (up to 2), background subtraction to reduce noise in final data, chromatographic data (minimum peak intensity of 500 cps), MS m/z tolerance (20 ppm; minimum intensity of 500 cps) and MS-MS tolerance (20 ppm; minimum intensity of 100 cps).

All data for potential metabolites generated were manually examined and interpreted. To verify the presence of metabolites identified, an extracted ion chromatogram (XIC) of each metabolite was generated in both MetabolitePilot™ and PeakView® and all MS-MS spectra were evaluated. After thorough data review and assessment of the practicality of all findings observed, the biotransformations, metabolite retention times, elemental compositions, measured accurate masses, mass error and suspected chemical structures were tabulated and are presented in this report.

Results

Mass spectral characterization of APP-CHMINACA

A peak in the chromatogram associated with APP-CHMINACA was observed at 9.53 minutes. A precursor accurate mass of m/z 405.2286 ($[M + H]^+$) and the elemental composition $C_{24}H_{28}N_4O_2$ were generated via high-resolution mass spectral analysis. The product ion mass spectrum and chemical structures of APP-CHMINACA and its most prominent fragments are presented in Figure 2. The base peak of the mass spectrum, nominal m/z 241, represents cleavage of the amide bond with the CHM-indazole acylium moiety remaining; m/z 145 corresponds to the indazole acylium ion; m/z 360 is indicative of the loss of the terminal amide group from the precursor structure; and m/z 388 represents loss of amine. The absence of these ions from the product ion spectra of proposed metabolites or a shift in mass (e.g., increase due to the addition of a new substituent) are indicative of biotransformation and was noted during metabolite characterization. The mass spectrum of APP-CHMINACA was consistent with those previously reported (23, 24).

Characterization of APP-CHMINACA metabolites

Twelve metabolites were identified in the study, spanning seven different chemical subclasses. Two major biotransformation pathways were observed; the first was hydrolysis of the distal amide moiety; the second, hydroxylation of the CHM ring. Hydrolyzed APP-CHMINACA was subsequently oxidized, generating products of mono- and dihydroxylation and ketone formation. Three APP-CHMINACA-specific metabolites were produced; one mono-, di- and trihydroxylated metabolite each was identified.

A summary of the main findings of the current study are presented in Table I. The characterization of each metabolite identified was conducted by evaluating the following: measured accurate precursor mass and calculated mass error (ppm), mass of product ions and their relation to the parent molecule fragments, elemental composition of precursor and fragments and retention time. The rank (relative abundance) was calculated by dividing the peak areas of each metabolite

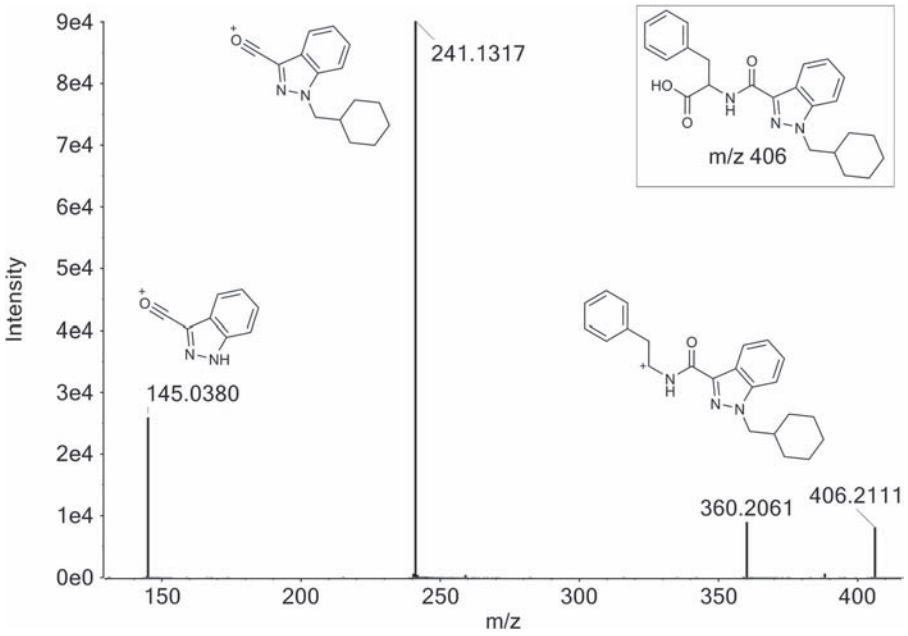

Figure 4. Product ion spectrum and chemical structures of M1 (top right) and fragment ions.

by the peak area of the most abundant metabolite. All data were consistent between each replicate—a requirement in order to make a positive identification. No metabolites were identified in the control sample that only contained APP-CHMINACA and buffer solution; this indicates that no hydrolysis occurred as a result of the buffer.

The retention characteristics of the metabolites identified are presented in Figure 3, an XIC. The product ion spectra, fragmentation pattern and chemical structures of the most abundant metabolites and an APP-CHMINACA-specific metabolite are presented in Figures 4–6. The precursor molecules and their nominal masses are enclosed in a text box in the figures to differentiate them from the proposed fragment structures. The fragment structures are adjacent to their representative peaks. Similar data for all other metabolites discussed are provided in the Supplementary Materials (Figures S1–S5).

The metabolic pathways proposed for APP-CHMINACA are presented in Figure 7. The exact site of biotransformation was not determined in the current study; potential sites are represented by Markush bonds. In order to elucidate the specific site, subsequent studies would need to be undertaken. Each metabolite and (as applicable) its isomers would need to be synthesized and analyzed chromatographically and via NMR spectroscopy to determine the absolute structure of each metabolite presented in this report.

M1: distal amide hydrolysis

The most abundant metabolite identified, M1, was a distal amide hydrolysis product with no further substitution. M1 had a retention time of 9.81 minutes, with a nominal precursor mass of m/z 406. This metabolite was approximately equal in abundance to APP-CHMINACA (Figure 3). The only structural difference between M1 and APP-CHMINACA is the presence of a terminal carboxylic acid group in place of amide. The main product ions of M1 were shared with APP-CHMINACA (Figure 4). M1 was also identified in the QC sample, indicating that it is an NADPH-independent biotransformation; this is a common occurrence among synthetic cannabinoids and other compounds possessing amide and ester functional groups (37–43).

M2: distal amide hydrolysis and monohydroxylation (CHM)

Five metabolites, M2.1–M2.5, were products of distal amide hydrolysis with monohydroxylation on the CHM moiety, each with a precursor mass of m/z 422. The metabolites eluted at 7.83, 8.00, 8.19, 8.44 and 8.54 minutes, respectively. M2.1 was present in the greatest abundance; overall, metabolites of this class were the most numerous of all metabolites identified. Hydroxylation on CHM was verified by the presence of representative ions in its product ion spectrum (Figure 5). Specifically, m/z 145 represented intact indazole; the base peak at m/z 257, an increase of m/z 16 (addition of O) relative to m/z 241 present in M1, represented monohydroxylation of CHM; and m/z 376, also an increase of m/z 16 relative to m/z 360 in the product ion spectrum of M1 (Figure 4), indicated monohydroxylation. The product ion spectrum presented in Figure 5 was observed for M2.1, M2.3 and M2.4; for metabolites M2.2 and M2.5, a similar spectrum was produced—m/z 145, 257 and 376 were present—but the base peak of the product ion spectrum was 239 instead of 257, indicative of the loss of water from the molecule (Figure S1).

M3: distal amide hydrolysis and ketone (CHM) formation

Two minor metabolites were generated, M3.1 and M3.2, that were products of distal amide hydrolysis with ketone formation on the CHM moiety. These were the result of further oxidation of M2, from hydroxyl to ketone. The precursor mass was m/z 420, and the metabolites had retention times of 7.96 and 8.04 minutes, respec-

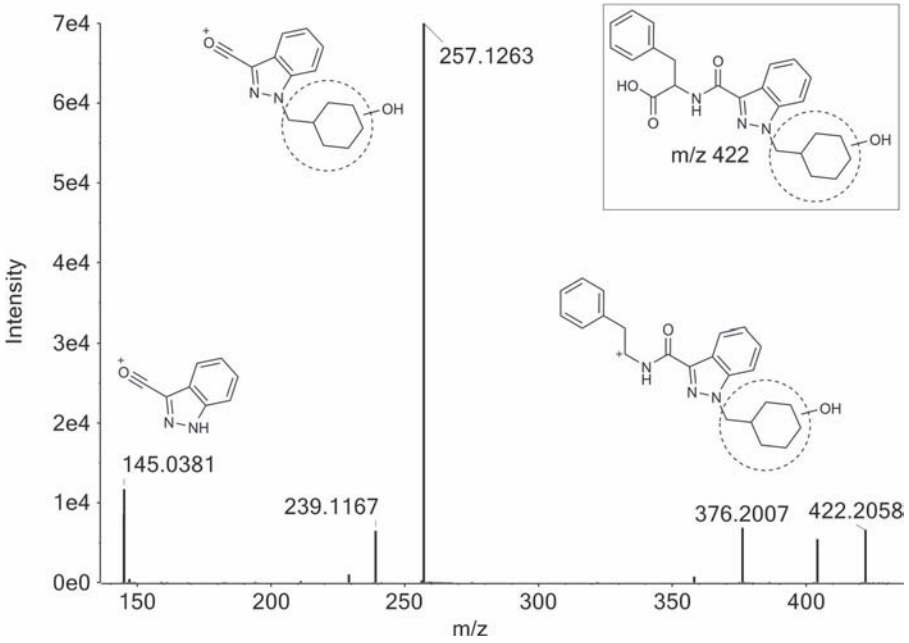

Figure 5. Product ion spectrum and chemical structures of M2 (top right) and fragment ions.

tively. The precursor mass was consistent with loss of 2H from M2, indicating the formation of a double bond. The presence of m/z 145 in the product ion spectrum (Figure S2) was indicative of intact indazole; m/z 255 (a decrease in mass of 2 relative to m/z 257 observed in M2) demonstrated the formation of a ketone; and m/z 374 further verified this finding, as it is also a decrease in mass of 2 relative to m/z 376 in M2.

M4: distal amide hydrolysis and dihydroxylation (CHM)

A minor metabolite, M4, that was the result of further hydroxylation of M2 eluted at 7.36 minutes; it was a distal amide hydrolysis metabolite with dihydroxylation on the CHM moiety and a mass of m/z 438. The m/z 145 ion, representing an intact indazole core group, was present in the product ion spectrum (Figure S3); dihydroxylation on CHM was proven by m/z 273, an increase in mass of 16 relative to m/z 257 found in the mass spectrum of M2 (Figure 5); m/z 420 represents the loss of water from the molecule.

M5: monohydroxylation (CHM)

A monohydroxylated minor metabolite specific to APP-CHMINACA, M5, was observed at 7.43 minutes and had a precursor mass of m/z 421. Representative fragments present in the product ion spectrum (Figure S4) were used to demonstrate that hydroxylation took place on the CHM moiety. Intact indazole was indicated by m/z 145; m/z 257 represented an increase of m/z 16 (gain of O) relative to m/z 241 present in the spectrum of APP-CHMINACA (Figure 2), indicating monohydroxylation; m/z 376 was also the result of a gain of m/z 16 in the m/z 360 fragment in APP-CHMINACA. M5 was the least abundant of all APP-CHMINACA-specific metabolites.

M6: dihydroxylation (CHM)

The most abundant APP-CHMINACA-specific metabolite, M6, was a dihydroxylation product, with hydroxylation occurring on the CHM group. The compound had a retention time of 6.62 minutes with a mass of m/z 437. Product ion m/z 273 in the mass spectrum (Figure 6) represented dihydroxylation of the CHM group; this was an increase of 16 and 32 mass units relative to m/z 257 and 241 observed in M5 and APP-CHMINACA, respectively. The ion m/z 392 was the result of further hydroxylation of the fragment associated with m/z 376 in M5 and dihydroxylation of the fragment of m/z 360 in APP-CHMINACA. The peaks at m/z 255 and 374 represent the loss of water from m/z 273 and m/z 392, respectively.

M7: trihydroxylation (CHM)

A minor, trihydroxylated metabolite, M7, with mass m/z 453 was observed at 6.47 minutes. This APP-CHMINACA-specific metabolite had characteristic ions that were indicative of trihydroxylation on the CHM moiety (Figure S5). A fragment of m/z 145 indicated that hydroxylation did not take place on indazole; m/z 289 represented trihydroxylation on CHM due to an m/z increase of 16 and 48 mass units relative to the related fragments at m/z 273 and m/z 241 present in the spectra of M6 and APP-CHMINACA, respectively. Trihydroxylation on CHM was further substantiated by the presence of m/z 408, an increase in mass of 16 and 48 relative to m/z 392 and m/z 360 in M6 and APP-CHMINACA, respectively.

Discussion

The HLM incubation and metabolite characterization procedures used in the current study have been successfully applied to the *in vitro* phase I metabolic profile elucidation of several classes of NPS. This includes multiple synthetic cannabinoids, opioid receptor agonists and cathinone and phenethylamine derivatives (36, 37, 44–48). Some studies accompanied *in vivo* confirmatory testing via LC-MS analysis of authentic human biological specimens; high correlations between major metabolites identified *in vitro* and those found *in vivo* were reported. These findings prove the broad applicability of the method

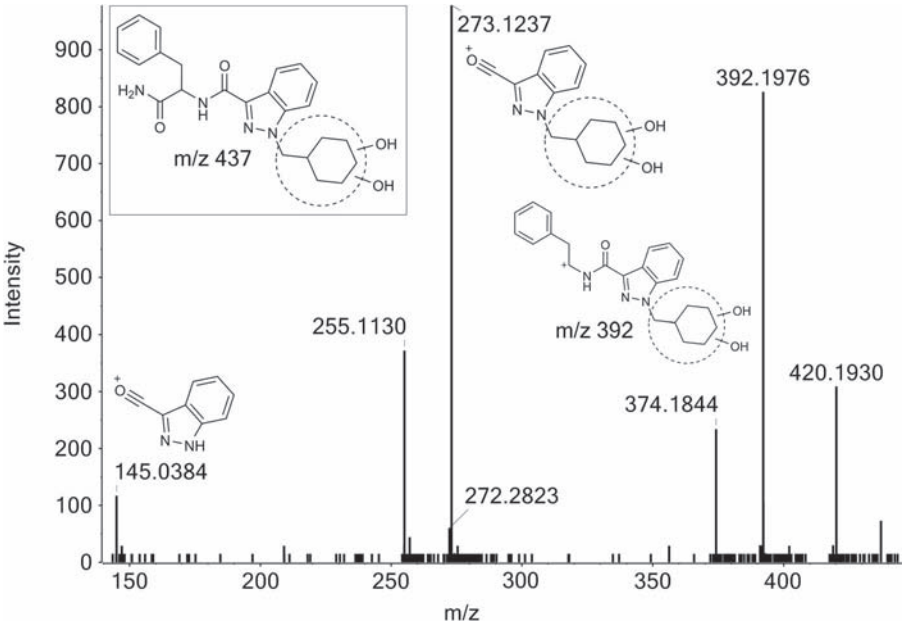

Figure 6. Product ion spectrum and chemical structures of M6 (top left) and fragment ions.

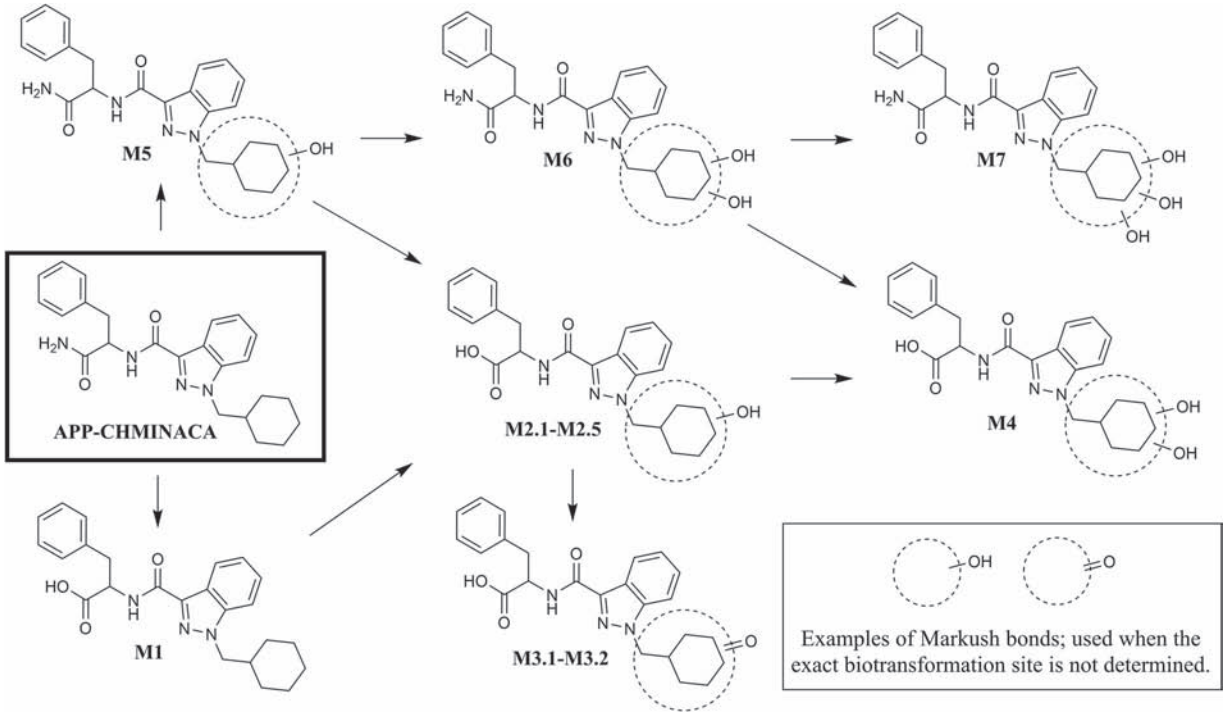

Figure 7. Proposed metabolic pathway of APP-CHMINACA.

to many chemical classes of compounds; the method is not limited to drugs of abuse and can also be used to determine the metabolic pathways of non-drug substances.

The metabolism of several indazole carboxamide synthetic cannabinoids has previously been determined and reported, including molecules containing a CHM substituent such as the following: AB-CHMICA, ADB-CHMICA (MAB-CHMICA), AB-CHMINACA, ADB-CHMINACA (MAB-CHMINACA), AMB-CHMICA, AMB-CHMINACA, MDMB-CHMICA and MDMB-CHMINACA (37–39, 41, 43, 49–58); the current work complements this collection of studies. It is essential that researchers continue to investigate the metabolic and toxicological processes associated with synthetic cannabinoids to develop a greater understanding of what occurs upon ingestion of these compounds and the effects they have on the body. Additionally, these studies allow reference material vendors to synthesize the appropriate markers of consumption so that method development scientists can produce assays for clinical and forensic applications.

Two major biotransformation pathways were associated with APP-CHMINACA metabolism; namely, hydrolysis of the terminal

amide group to carboxylic acid and hydroxylation of the CHM moiety. These biotransformations are consistent with those reported for structurally related synthetic cannabinoids, including those tested by the authors (36, 37, 39–41, 52). The metabolites identified in the greatest abundance were a distal amide hydrolysis product with no further biotransformation (M1) and a related metabolite featuring distal amide hydrolysis with hydroxylation on the CHM ring (M2.1). APP-CHMINACA-specific metabolites were identified, with a CHM-dihydroxylated product (M6) present in the greatest abundance. The authors propose that these three metabolites are the best markers for confirming consumption of APP-CHMINACA in human biological specimens. To the authors' knowledge, there is currently no synthetic cannabinoid that shares these metabolites, allowing for distinguishing between consumption of APP-CHMINACA and other compounds. The metabolites identified in the current study are consistent with those identified and included in the testing scope established by Staeheli *et al.* (59).

In general, the major metabolic pathway of synthetic cannabinoids is hydroxylation facilitated by cytochrome P450 (CYP450) enzymes (5, 60, 61); in addition to hydroxylation, compounds possessing amide and ester groups typically undergo hydrolysis, facilitated by carboxylesterase (CES) or amidase enzymes (38, 42). Both of these enzymes are present in HLM, making them useful for *in vitro* metabolism determinations (62).

APP-CHMINACA metabolized similarly to MDMB-CHMINACA, which also possesses a CHM group and was tested via the same incubation procedure (37). The two compounds shared the same major metabolic routes (hydrolysis and hydroxylation), though MDMB-CHMINACA possesses a terminal ester instead of amide. In the case of APP-CHMINACA, the prominent metabolites were amide hydrolysis products, the most abundant being hydrolyzed with no further biotransformation. Hydroxylations on APP-CHMINACA all occurred on the CHM ring and included mono-, di- and trihydroxylation. For MDMB-CHMINACA, the most abundant metabolite was monohydroxylated on CHM. A CHM-dihydroxylated product was also generated for MDMB-CHMINACA, but no trihydroxylation took place. Like APP-CHMINACA, the main ester hydrolysis product also had no further biotransformation (37).

APP-CHMINACA is structurally related to PX-1 (5F-APP-PICA) and shared some metabolic features; the two compounds were evaluated using identical procedures (36). The greatest degree of consistency observed between the two compounds was hydrolysis of the terminal amide group (APP moiety) as one of the most abundant metabolites; unlike PX-1, no hydroxylation of the benzyl group occurred for APP-CHMINACA. Since PX-1 possesses a fluoropentyl side chain, it metabolizes differently than CHM-containing synthetic cannabinoids, including defluorination/hydroxylation on the chain and *N*-dealkylation as major products (36).

Additional studies on APP-CHMINACA and other synthetic cannabinoids with limited pharmacological data are warranted. These include evaluations of their pharmacokinetic and pharmacodynamic properties, *in vitro* assays to determine the pharmacological activity of the metabolites identified in metabolism studies and assessments on their interactions with metabolic enzymes. Though carboxylic acid metabolites of synthetic cannabinoids have shown little to no activity at the CB receptors, many hydroxylated metabolites have proven to be receptor agonists, inducing greater effects than THC (60, 63–70). Some synthetic cannabinoids even inhibit drug-metabolizing enzymes, potentially leading to severe toxic effects (71). These studies would serve to create a link between the initial identification of synthetic cannabinoids in forensic casework, determination of their metabolic pathway and toxicologic effects and assessing the effects that synthetic cannabinoids and related NPS have on humans.

Conclusions

This publication provides the detailed *in vitro* phase I metabolic profile of the CHM indazole carboxamide synthetic cannabinoid APP-CHMINACA (PX-3). Following incubation with HLM, 12 metabolites were generated and characterized via HRMS, using a UHPLC-QTOF-MS platform. The predominant biotransformations that occurred in the study were hydrolysis of the distal amide moiety and hydroxylation of the CHM substituent. The metabolites present in the greatest abundance were a distal amide hydrolysis product with no further biotransformation (M1) and a related metabolite, distal amide hydrolysis with hydroxylation on the CHM ring (M2.1). Hydroxylated metabolites specific to APP-CHMINACA were also identified, with CHM-dihydroxylation (M6) as the most prominent. The authors therefore propose that the most appropriate markers for confirming consumption of APP-CHMINACA are M1, M2.1 and M6; though M1 and M2.1 are more abundant than M6, it can be used to unequivocally determine APP-CHMINACA ingestion. The classes of metabolites identified in the current study are consistent with those reported for related synthetic cannabinoids, specifically those with CHM substituents and distal amide groups. Application of the HLM incubation procedure, mass spectral data collection parameters and the metabolite characterization process described in this study demonstrates the utility of the method, as it has been used to identify the *in vitro* metabolic pathways of multiple synthetic cannabinoids as well as other classes of NPSs.

References

1. Banister, S.D., Connor, M. (2018) The chemistry and pharmacology of synthetic cannabinoid receptor agonists as new psychoactive substances: origins. *Handbook of Experimental Pharmacology*, 252, 165–190.
2. Abbate, V., Schwenk, M., Presley, B.C., Uchiyama, N. (2018) The ongoing challenge of novel psychoactive drugs of abuse. Part I. Synthetic cannabinoids (IUPAC Technical Report). *Pure and Applied Chemistry*, 90, 1255–1282.
3. Auwärter, V., Dresen, S., Weinmann, W., Müller, M., Pütz, M., Ferreirós, N. (2009) 'Spice' and other herbal blends: harmless incense or cannabinoid designer drugs? *Journal of Mass Spectrometry*, 44, 832–837.
4. Lindigkeit, R., Boehme, A., Eiserloh, I., Luebbecke, M., Wiggermann, M., Ernst, L. *et al.* (2009) Spice: a never ending story? *Forensic Science International*, 191, 58–63.
5. Presley, B.C., Gurney, S.M.R., Scott, K.S., Kacinko, S.L., Logan, B.K. (2016) Metabolism and toxicological analysis of synthetic cannabinoids in biological fluids and tissues. *Forensic Science Review*, 28, 103–169.
6. Wadsworth, E., Drummond, C., Deluca, P. (2018) The dynamic environment of crypto markets: the lifespan of new psychoactive substances (NPS) and vendors selling NPS. *Brain Sciences*, 8, e46–e54.
7. Presley, B.C., Jansen-Varnum, S.A., Logan, B.K. (2013) Analysis of synthetic cannabinoids in botanical material: a review of analytical methods and findings. *Forensic Science Review*, 25, 27–46.
8. *United Nations Office on Drugs and Crime World Drug Report 2018: Booklet 3—Analysis of Drug Markets: Opiates, Cocaine, Cannabis, Synthetic Drugs*. https://www.unodc.org/pdf/opioids-crisis/WDR18_Booklet_3_DRUG_MARKETS.pdf (accessed June 20, 2019).
9. Tettey, J.N.A., Crean, C., Ifeagwu, S.C., Raithelhuber, M. Emergence, diversity, and control of new psychoactive substances: a global perspective. In: Maurer H.H., Brandt S.D. (eds). *New Psychoactive Substances:*

Pharmacology, Clinical, Forensic and Analytical Toxicology. Springer International Publishing: Switzerland, 2018; pp51–67.
10. *United Nations Office on Drugs and Crime Current NPS Threats: Volume I, March 2019*. https://www.unodc.org/LSS/Announcement/Details/0bd37fbb-112a-4210-a52c-a0279483ae5d (accessed June 20, 2019).
11. Antonides, L.H., Cannaert, A., Norman, C., Vives, L., Harrison, A., Costello, A. *et al.* (2019) Enantiospecific synthesis, chiral separation, and biological activity of four indazole-3-carboxamide-type synthetic cannabinoid receptor agonists and their detection in seized drug samples. *Frontiers in Chemistry*, 7. doi: 10.3389/fchem.2019.00321.
12. *Drug Enforcement Administration Emerging Threat Report: Annual 2018*. https://ndews.umd.edu/sites/ndews.umd.edu/files/Emerging-Threat-Report-2018-Annual.pdf (accessed June 20, 2019).
13. *Center for Forensic Science Research and Education, NPS Discovery—Trend Report: Q4 2018: Synthetic Cannabinoids in the United States 2018*. https://www.forensicscienceeducation.org/wp-content/uploads/2019/02/Synthetic-Cannabinoid-Trend-Report_Detailed_2018-Q4.pdf (accessed June 20, 2019).
14. Angerer, V., Jacobi, S., Franz, F., Auwärter, V., Pietsch, J. (2017) Three fatalities associated with the synthetic cannabinoids 5F-ADB, 5F-PB-22, and AB-CHMINACA. *Forensic Science International*, 281, e9–e15.
15. Barceló, B., Pichini, S., López-Corominas, V., Gomila, I., Yates, C., Busardò, F.P. *et al.* (2017) Acute intoxication caused by synthetic cannabinoids 5F-ADB and MMB-2201: a case series. *Forensic Science International*, 273, e10–e14.
16. Gurney, S.M.R., Scott, K.S., Kacinko, S.L., Presley, B.C., Logan, B.K. (2014) Pharmacology, toxicology, and adverse effects of synthetic cannabinoid drugs. *Forensic Science Review*, 26, 53–78.
17. Koller, V.J., Ferk, F., Al-Serori, H., Mišík, M., Nersesyan, A., Auwärter, V. *et al.* (2015) Genotoxic properties of representatives of alkylindazoles and aminoalkyl-indoles which are consumed as synthetic cannabinoids. *Food and Chemical Toxicology*, 80, 130–136.
18. Rianprakaisang, T., Gerona, R., Hendrickson, R.G. (2019) Commercial cannabidiol oil contaminated with the synthetic cannabinoid AB-FUBINACA given to a pediatric patient. *Clinical Toxicology*. doi: 10.1080/15563650.2019.1619758.
19. Banister, S.D., Longworth, M., Kevin, R., Sachdev, S., Santiago, M., Stuart, J. *et al.* (2016) Pharmacology of valinate and tert-leucinate synthetic cannabinoids 5F-AMBICA, 5F-AMB, 5F-ADB, AMB-FUBINACA, MDMB-FUBINACA, MDMB-CHMICA, and their analogues. *ACS Chemical Neuroscience*, 7, 1241–1254.
20. Schoeder, C.T., Hess, C., Madea, B., Meiler, J., Müller, C.E. (2018) Pharmacological evaluation of new constituents of 'Spice': synthetic cannabinoids based on indole, indazole, benzimidazole and carbazole scaffolds. *Forensic Toxicology*, 36, 385–403.
21. Buchler, I., Hayes, M., Hegde, S., Hockerman, S., Jones, D., Kortum, S., *et al. Indazole Derivatives: Patent WO/2009/106980*. https://patentscope.wipo.int/search/en/detail.jsf?docId=WO2009106980 (accessed June 20, 2019).
22. Doi, T., Tagami, T., Takeda, A., Asada, A., Sawabe, Y. (2018) Evaluation of carboxamide-type synthetic cannabinoids as CB1/CB2 receptor agonists: difference between the enantiomers. *Forensic Toxicology*, 36, 51–60.
23. Lobo Vicente, J., Chassaigne, H., Holland, M.V., Reniero, F., Kolář, K., Tirendi, S. *et al.* (2016) Systematic analytical characterization of new psychoactive substances: a case study. *Forensic Science International*, 265, 107–115.
24. *National Forensic Laboratory of Slovenia Analytical Report: APP-CHMINACA*. https://www.policija.si/apps/nfl_response_web/0_Analytical_Reports_final/APP-CHMINACA_(PX3)-ID-1280-15-report_final.pdf (accessed June 20, 2019).
25. Springer, Y.P., Gerona, R., Scheunemann, E., Shafer, S.L., Lin, T., Banister, S.D. *et al.* (2016) Increase in adverse reactions associated with use of synthetic cannabinoids—Anchorage, Alaska, 2015–2016. *MMWR. Morbidity and Mortality Weekly Report*, 65, 1108–1111.
26. Hess, C., Krueger, L., Unger, M., Madea, B. (2017) Freeze-thaw stability and long-term stability of 84 synthetic cannabinoids in serum. *Drug Testing and Analysis*, 9, 1506–1511.
27. Hess, C., Murach, J., Krueger, L., Scharrenbroch, L., Unger, M., Madea, B. *et al.* (2017) Simultaneous detection of 93 synthetic cannabinoids by liquid chromatography-tandem mass spectrometry and retrospective application to real forensic samples. *Drug Testing and Analysis*, 9, 721–733.
28. *Drug Enforcement Administration National Forensic Laboratory Information System Special Report: Synthetic Cannabinoids and Synthetic Cathinones Reported in NFLIS, 2013–2015*. https://www.nflis.deadiversion.usdoj.gov/DesktopModules/ReportDownloads/Reports/NFLIS-SR-SynthCannabinoidCathinone.pdf (accessed June 20, 2019).
29. *EMCDDA–Europol 2014 Annual Report on the implementation of Council Decision 2005/387/JHA*. http://www.emcdda.europa.eu/system/files/publications/1018/TDAN15001ENN.pdf (accessed June 20, 2019).
30. *Drug Enforcement Administration Drug Enforcement Administration Emerging Threat Report: Annual 2017*. https://ndews.umd.edu/sites/ndews.umd.edu/files/dea-emerging-threat-report-2017-annual.pdf (accessed June 20, 2019).
31. Altintop, I., Karakukcu, C. (2018) The chameleon-like properties of psychoactive drugs: examinations with HR LC- technology of patients presenting at the Emergency Department following the use of synthetic cannabinoids: a case series and literature review. *Behavioral Sciences*, 8, e88–e96.
32. Qian, Z., Jia, W., Li, T., Hua, Z., Liu, C. (2017) Identification and analytical characterization of four synthetic cannabinoids ADB-BICA, NNL-1, NNL-2, and PPA(N)-2201. *Drug Testing and Analysis*, 9, 51–60.
33. UNODC Early Warning Advisory (EWA) on New Psychoactive Substances (NPS). https://www.unodc.org/LSS/Home/NPS (accessed June 20, 2019).
34. *Center for Forensic Science Research and Education, NPS Discovery Report—APP-BINACA*. https://www.forensicscienceeducation.org/wp-content/uploads/2019/03/APP-BINACA_030619_CFSRE_Report.pdf (accessed June 20, 2019).
35. *Center for Forensic Science Research and Education, NPS Discovery Report—5F-MPP-PICA*. https://www.forensicscienceeducation.org/wp-content/uploads/2019/02/5F-MPP-PICA_021319_NMSLabs_Report.pdf (accessed June 20, 2019).
36. Presley, B.C., Logan, B.K., Jansen-Varnum, S.A. Phase I Metabolism of Synthetic Cannabinoid Receptor Agonist PX-1 (5F-APP-PICA) via Incubation with Human Liver Microsomes and UHPLC-HRMS; 2019. (Submitted for peer-review).
37. Presley, B.C., Logan, B.K., Jansen-Varnum, S.A. In vitro phase I metabolism of indazole carboxamide synthetic cannabinoid MDMB-CHMINACA via human liver microsome incubation and high-resolution mass spectrometry. *Drug Testing and Analysis*, 11, 1264–1276. doi: 10.1002/dta.2615.
38. Thomsen, R., Nielsen, L.M., Holm, N.B., Rasmussen, H.B., Linnet, K., INDICES Consortium (2015) Synthetic cannabimimetic agents metabolized by carboxylesterases. *Drug Testing and Analysis*, 7, 565–576.
39. Erratico, C., Negreira, N., Norouzizadeh, H., Covaci, A., Neels, H., Maudens, K. *et al.* (2015) In vitro and in vivo human metabolism of the synthetic cannabinoid AB-CHMINACA. *Drug Testing and Analysis*, 7, 866–876.
40. Franz, F., Angerer, V., Moosmann, B., Auwärter, V. (2017) Phase I metabolism of the highly potent synthetic cannabinoid MDMB-CHMICA and detection in human urine samples. *Drug Testing and Analysis*, 9, 744–753.
41. Franz, F., Jechle, H., Wilde, M., Angerer, V., Huppertz, L.M., Longworth, M. *et al.* (2019) Structure-metabolism relationships of valine and tert-leucine-derived synthetic cannabinoid receptor agonists: a systematic comparison of the in vitro phase I metabolism using pooled human liver microsomes and high-resolution mass spectrometry. *Forensic Toxicology*, 37, 316–329. doi: 10.1007/s11419-018-00462-x.
42. Lee, M.S., Zhu, M. *Mass Spectrometry in Drug Metabolism and Disposition: Basic Principles and Applications*. Hoboken, NJ, USA: John Wiley & Sons, 2011.
43. Takayama, T., Suzuki, M., Todoroki, K., Inoue, K., Min, J.Z., Kikura-Hanajiri, R. *et al.* (2014) UPLC/ESI–based determination of metabolism of several new illicit drugs, ADB-FUBINACA,

AB-FUBINACA, AB-PINACA, QUPIC, 5F-QUPIC and α-PVT, by human liver microsome. *Biomedical Chromatography*, 28, 831–838.
44. Krotulski, A.J., Papsun, D.M., De Martinis, B.S., Mohr, A.L.A., Logan, B.K. (2018) N-ethyl Pentylone (Ephylone) intoxications: Quantitative confirmation and metabolite identification in authentic human biological specimens. *Journal of Analytical Toxicology*, 42, 467–475. doi: 10.1093/jat/bky025.
45. Krotulski, A.J., Mohr, A.L.A., Papsun, D.M., Logan, B.K. (2018) Metabolism of novel opioid agonists U-47700 and U-49900 using human liver microsomes with confirmation in authentic urine specimens from drug users. *Drug Testing and Analysis*, 10, 127–136.
46. Krotulski, A.J., L A Mohr, A., Papsun, D.M., Logan, B.K. (2018) Dibutylone (bk-DMBDB): intoxications, quantitative confirmations and metabolism in authentic biological specimens. *Journal of Analytical Toxicology*, 42, 437–445. doi: 10.1093/jat/bky022.
47. Krotulski, A.J., Papsun, D.M., Friscia, M., Swartz, J.L., Holsey, B.D., Logan, B.K. (2018) Fatality following ingestion of tetrahydrofuranylfentanyl, U-49900 and methoxy-phencyclidine. *Journal of Analytical Toxicology*, 42, e27–e32.
48. Temporal, K.-D.H., Scott, K.S., Mohr, A.L.A., Logan, B.K. (2017) Metabolic profile determination of NBOMe compounds using human liver microsomes and comparison with findings in authentic human blood and urine. *Journal of Analytical Toxicology*, 41, 646–657.
49. Carlier, J., Diao, X., Sempio, C., Huestis, M.A. (2017) Identification of new synthetic cannabinoid ADB-CHMINACA (MAB-CHMINACA) metabolites in human hepatocytes. *The AAPS Journal*, 19, 568–577.
50. Castaneto, M.S., Wohlfarth, A., Pang, S., Zhu, M., Scheidweiler, K.B., Kronstrand, R. *et al.* (2015) Identification of AB-FUBINACA metabolites in human hepatocytes and urine using high-resolution mass spectrometry. *Forensic Toxicology*, 33, 295–310.
51. Gandhi, A.S., Zhu, M., Pang, S., Wohlfarth, A., Scheidweiler, K.B., Liu, H.-F. *et al.* (2013) First characterization of AKB-48 metabolism, a novel synthetic cannabinoid, using human hepatocytes and high-resolution mass spectrometry. *The AAPS Journal*, 15, 1091–1098.
52. Hasegawa, K., Minakata, K., Gonmori, K., Nozawa, H., Yamagishi, I., Watanabe, K. *et al.* (2018) Identification and quantification of predominant metabolites of synthetic cannabinoid MAB-CHMINACA in an authentic human urine specimen. *Drug Testing and Analysis*, 10, 365–371.
53. Kusano, M., Zaitsu, K., Taki, K., Hisatsune, K., Nakajima, J., Moriyasu, T. *et al.* (2018) Fatal intoxication by 5F–ADB and diphenidine: detection, quantification, and investigation of their main metabolic pathways in humans by LC/ and LC/Q-TOFMS. *Drug Testing and Analysis*, 10, 284–293.
54. Öztürk, Y.E., Yeter, O., Öztürk, S., Karakus, G., Ates, I., Buyuk, Y. *et al.* (2018) Detection of metabolites of the new synthetic cannabinoid CUMYL-4CN-BINACA in authentic urine samples and human liver microsomes using high-resolution mass spectrometry. *Drug Testing and Analysis*, 10, 449–459.
55. Yeter, O., Erol Öztürk, Y. (2019) Metabolic profiling of synthetic cannabinoid 5F-ADB by human liver microsome incubations and urine samples using high-resolution mass spectrometry. *Drug Testing and Analysis*, 11, 847–858. doi: 10.1002/dta.2566.
56. Staeheli, S.N., Poetzsch, M., Veloso, V.P., Bovens, M., Bissig, C., Steuer, A.E. *et al.* (2018) In vitro metabolism of the synthetic cannabinoids CUMYL-PINACA, 5F-CUMYL-PINACA, CUMYL-4CN-BINACA, 5F-CUMYL-P7AICA and CUMYL-4CN-B7AICA. *Drug Testing and Analysis*, 10, 148–157.
57. Wohlfarth, A., Castaneto, M.S., Zhu, M., Pang, S., Scheidweiler, K.B., Kronstrand, R. *et al.* (2015) Pentylindole/Pentylindazole synthetic cannabinoids and their 5-fluoro analogs produce different primary metabolites: Metabolite profiling for AB-PINACA and 5F-AB-PINACA. *The AAPS Journal*, 17, 660–677.
58. Kavanagh, P., Grigoryev, A., Krupina, N. (2017) Detection of metabolites of two synthetic cannabimimetics, MDMB-FUBINACA and ADB-FUBINACA, in authentic human urine specimens by accurate mass LC–MS: a comparison of intersecting metabolic patterns. *Forensic Toxicology*, 35, 284–300.
59. Staeheli, S.N., Veloso, V.P., Bovens, M., Bissig, C., Kraemer, T., Poetzsch, M. LC-MS/MS screening method using information-dependent acquisition of enhanced product ion mass spectra for synthetic cannabinoids including metabolites in urine. *Drug Testing and Analysis*, 11, 1369–1376 . doi: 10.1002/dta.2664.
60. Chimalakonda, K.C., Seely, K.A., Bratton, S.M., Brents, L.K., Moran, C.L., Endres, G.W. *et al.* (2012) Cytochrome P450-mediated oxidative metabolism of abused synthetic cannabinoids found in K2/Spice: identification of novel cannabinoid receptor ligands. *Drug Metabolism and Disposition*, 40, 2174–2184.
61. Sobolevsky, T., Prasolov, I., Rodchenkov, G. (2012) Detection of urinary metabolites of AM-2201 and UR-144, two novel synthetic cannabinoids. *Drug Testing and Analysis*, 4, 745–753.
62. Asha, S., Vidyavathi, M. (2010) Role of human liver microsomes in in vitro metabolism of drugs-a review. *Applied Biochemistry and Biotechnology*, 160, 1699–1722.
63. Wouters, E., Mogler, L., Cannaert, A., Auwärter, V., Stove, C. Functional evaluation of carboxy metabolites of synthetic cannabinoid receptor agonists featuring scaffolds based on L-valine or L-tert-leucine. *Drug Testing and Analysis*, 11, 1183–1191. doi: 10.1002/dta.2607.
64. Brents, L.K., Reichard, E.E., Zimmerman, S.M., Moran, J.H., Fantegrossi, W.E., Prather, P.L. (2011) Phase I hydroxylated metabolites of the K2 synthetic cannabinoid JWH-018 retain in vitro and in vivo cannabinoid 1 receptor affinity and activity. *PloS One*, 6, e21917.
65. Brents, L.K., Gallus-Zawada, A., Radominska-Pandya, A., Vasiljevik, T., Prisinzano, T.E., Fantegrossi, W.E. *et al.* (2012) Monohydroxylated metabolites of the K2 synthetic cannabinoid JWH-073 retain intermediate to high cannabinoid 1 receptor (CB1R) affinity and exhibit neutral antagonist to partial agonist activity. *Biochemical Pharmacology*, 83, 952–961.
66. Gamage, T.F., Farquhar, C.E., McKinnie, R.J., Kevin, R.C., McGregor, I.S., Trudell, M. *et al.* (2018) Synthetic cannabinoid hydroxypentyl metabolites retain efficacy at human cannabinoid receptors. *The Journal of Pharmacology and Experimental Therapeutics*, 368, 414–422. doi: 10.1124/jpet.118.254425.
67. Cannaert, A., Storme, J., Hess, C., Auwärter, V., Wille, S.M.R., Stove, C.P. (2018) Activity-based detection of cannabinoids in serum and plasma samples. *Clinical Chemistry*, 64, 918–926.
68. Cannaert, A., Franz, F., Auwärter, V., Stove, C.P. (2017) Activity-based detection of consumption of synthetic cannabinoids in authentic urine samples using a stable cannabinoid reporter system. *Analytical Chemistry*, 89, 9527–9536.
69. Noble, C., Cannaert, A., Linnet, K., Stove, C.P. (2019) Application of an activity-based receptor bioassay to investigate the in vitro activity of selected indole- and indazole-3-carboxamide-based synthetic cannabinoids at CB1 and CB2 receptors. *Drug Testing and Analysis*, 11, 501–511.
70. Couceiro, J., Bandarra, S., Sultan, H., Bell, S., Constantino, S., Quintas, A. (2016) Toxicological impact of JWH-018 and its phase I metabolite N-(3-hydroxypentyl) on human cell lines. *Forensic Science International*, 264, 100–105.
71. Kong, T.Y., Kim, J.-H., Kim, D.K., Lee, H.S. (2018) Synthetic cannabinoids are substrates and inhibitors of multiple drug-metabolizing enzymes. *Archives of Pharmacal Research*, 41, 691–710. doi: 10.1007/s12272-018-1055-x.